



LAWRENCE
LIVERMORE
NATIONAL
LABORATORY

Experimental Validation of the Methodology for Partial Defect Verification of the Pressurized Water Reactor Spent Fuel Assemblies

Y. S. Ham, S. Sitaraman, H. Shin, S. Eom, H. Kim

June 16, 2009

INMM 50th Annual Meeting
Tucson, AZ, United States
July 12, 2009 through July 16, 2009

Disclaimer

This document was prepared as an account of work sponsored by an agency of the United States government. Neither the United States government nor Lawrence Livermore National Security, LLC, nor any of their employees makes any warranty, expressed or implied, or assumes any legal liability or responsibility for the accuracy, completeness, or usefulness of any information, apparatus, product, or process disclosed, or represents that its use would not infringe privately owned rights. Reference herein to any specific commercial product, process, or service by trade name, trademark, manufacturer, or otherwise does not necessarily constitute or imply its endorsement, recommendation, or favoring by the United States government or Lawrence Livermore National Security, LLC. The views and opinions of authors expressed herein do not necessarily state or reflect those of the United States government or Lawrence Livermore National Security, LLC, and shall not be used for advertising or product endorsement purposes.

Experimental Validation of the Methodology for Partial Defect Verification of the Pressurized Water Reactor Spent Fuel Assemblies

Young S. Ham and Shivakumar Sitaraman

Lawrence Livermore National Laboratory, Livermore, CA

Heesung Shin, Sungho Eom and Hodong Kim

Korea Atomic Energy Research Institute, Daejeon, Korea

E-mail address of main author: ham4@llnl.gov

ABSTRACT

A set of controlled experiments and Monte Carlo simulation studies with actual commercial pressurized water reactor (PWR) spent fuel assemblies were performed in order to validate an earlier proposal for partial defect testing of the PWR spent fuel assemblies. The proposed methodology involved insertion of tiny neutron and gamma detectors into the guide tubes of PWR assemblies, measurements and data evaluation. One of the key features of the data evaluation method was the concept of the base signature obtained by normalizing the ratio of gamma to neutron signals at each measurement position. As the base signature is relatively invariant to the characteristic variations of spent fuel assemblies such as initial fuel enrichment, cooling time, and burn-up, the methodology could be a powerful verification method which does not require operator declared information on the spent fuel. The benchmarking experiments indeed demonstrated that the methodology can be used for partial defect verification of the PWR spent fuel assemblies without operator declared data. The results from the experiments were compared with the simulations and the agreement between the two was well within ten percent. Thus, based on the simulation studies and benchmarking measurements, the methodology developed promises to be a powerful and practical way to detect partial defects that constitute 10% or more of the total active fuel pins. This far exceeds the detection threshold of 50% missing pins from a spent fuel assembly, a threshold defined by the IAEA Safeguards Criteria.

INTRODUCTION

A new safeguards method and an associated instrument, Partial Defect Detector (PDET), are under development at LLNL for partial defect verification of spent fuel assemblies [1-5]. The new measurement methodology uses multiple tiny neutron and gamma detectors in a form of cluster and high precision driving system to obtain underwater radiation measurements inside a Pressurized Water Reactor (PWR) spent fuel assembly. The method takes advantage of the PWR fuel design which contains multiple guide tubes which can be accessed from the top. The data obtained in such a manner can provide spatial distribution of neutron and gamma flux within a spent fuel assembly. Our simulation study indicated that the ratio of the gamma signal to the thermal neutron signal at each detector location normalized to the peak ratio of all the detector locations gives a unique signature that is sensitive to missing pins. The signature is principally dependent on the geometry of the detector locations, and little sensitivity to enrichment variations or burn-ups. A small variation in the fuel bundle such as a few missing pins changes the shape of the signature to enable detection. This resulted in a breakthrough method which can be used to detect pin diversion without relying on the nuclear power plant operator's declared operation data. In addition, the integrated neutron signal and gamma signal can be used in to verify the consistency of the operator declaration on the fuel burn-ups and cooling times.

BENCHMARKING EXPERIMENTS

The three spent fuel assemblies used for benchmarking measurements, discharged from an actual commercial PWR nuclear power plant, Kori-1, in Korea are currently being stored at Korea Atomic Energy Research Institute with the top nozzle removed. Basic information on the three Westinghouse 14 x 14 fuel assemblies is presented in Table 1. Figures 1-3 show the location of fuel rod, control rod guide tube and instrumentation tube for the assemblies C15, G23 and J14. Although all fuel rods were present at the time of discharge, since then many fuel rods have been removed for destructive testing. Twenty two fuel rods each were removed from assemblies C15 and G23, corresponding to 12% of the total number of fuel rods (179) in an assembly. The positions where the fuel rods were removed are shown in red and are filled with water. In addition, three rods were replaced by stainless steel rods in G23 (indicated by the “stars” in Figure 2). Thus, the assembly G23 has approximately 14% of the fuel rods missing. The assembly J14 has only one fuel rod missing and essentially represented a full assembly. It must be noted that the Westinghouse type 14x14 is not totally symmetric due to the presence of the instrumentation tube, which is filled with water, at the position G7. Figures 4-6 show pin-by-pin fuel rod burn-up distributions for C15, G23 and J14 assemblies. The assemblies C15 and G23 have steep gradients of fuel burn-up, i.e., the difference in burn-up between the lowest and the highest for C15 and G23 were 35 % and 80%, respectively. The extent of the variation in G23 is unusual and represents an extreme case to test the validity of the PDET methodology.

Table 1: Description of the three PWR spent fuel assemblies used for experiments.

Fuel ID	Fuel Type	Burnup (GWd/tU)	Discharge Date	Initial Enrichment (%)	Number of missing rods
C15	WH 14x14	32.0	4/17/82	3.2	22 (12%)
G23	WH 14x14	35.5	10/24/86	3.2	25 (14%)
J14	WH 14x14	37.5	1/20/89	3.2	1 (0.6 %)

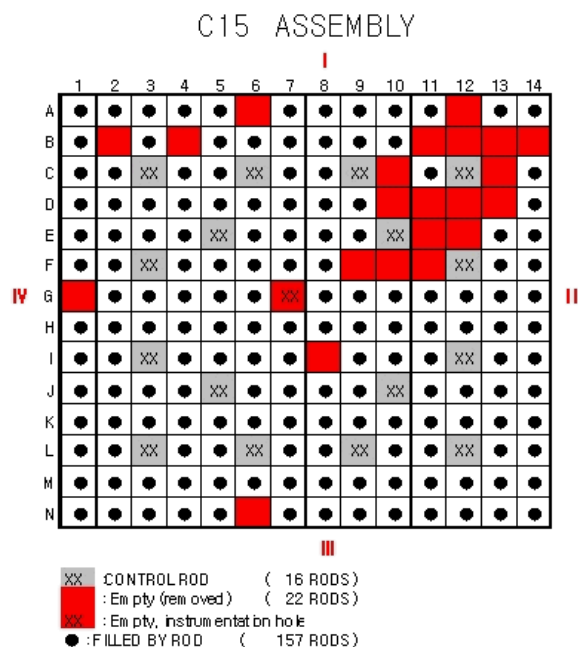


Figure 1: Map showing the location of the fuel rods, control rod holes and instrumentation hole for the spent fuel assembly C15. The blocks colored red indicates position covered with water.

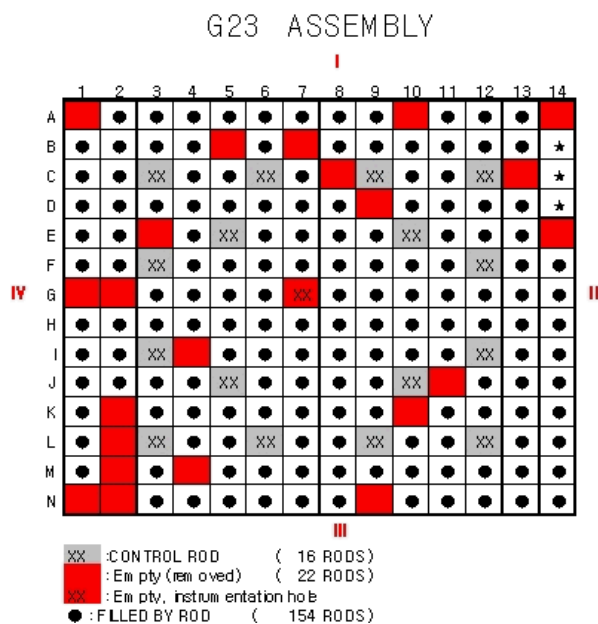


Figure 2: Map showing the location of the fuel rods, control rod holes and instrumentation hole for the spent fuel assembly G23. The blocks colored red indicates position covered with water.

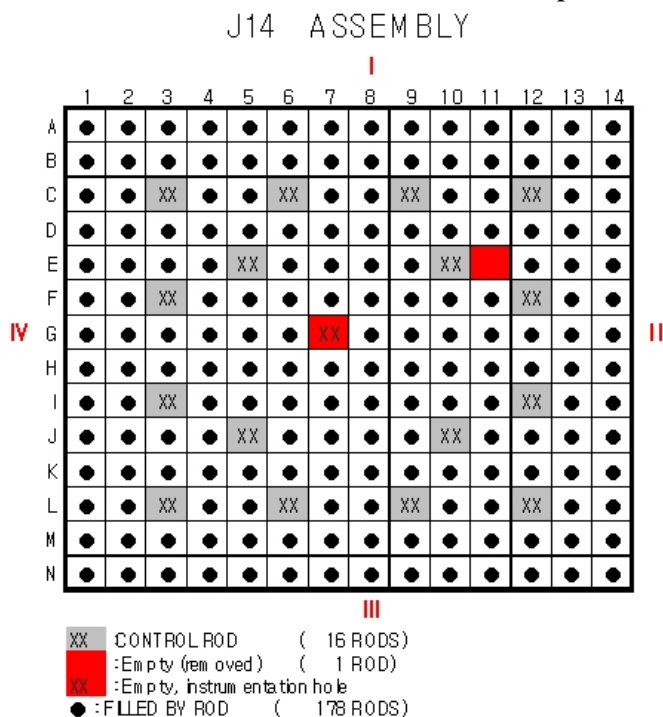


Figure 3: Map showing the location of the fuel rods, control rod holes and instrumentation hole for the spent fuel assembly J14. The blocks colored red indicates position covered with water.

	1	2	3	4	5	6	7	8	9	10	11	12	13	14
A	29.9	29.9	29.9	32.0	32.0	32.0	32.8	32.8	33.6	33.6	33.6	34.2	34.2	34.2
B	29.9	31.7	31.7	31.7	33.2	33.2	34.0	34.0	34.9	34.9	35.1	35.1	35.1	34.2
C	29.9	31.7	xx	33.6	33.6	xx	34.0	34.0	xx	35.8	35.8	xx	35.1	34.2
D	29.9	31.7	33.6	33.6	33.6	33.6	34.0	34.0	35.8	35.8	35.8	35.8	35.1	33.9
E	29.9	31.8	33.6	33.6	xx	33.6	33.1	33.1	35.8	xx	35.8	35.8	35.1	33.9
F	29.9	31.8	xx	33.6	33.6	33.6	33.1	33.1	35.8	35.8	35.8	xx	35.1	33.9
G	28.3	31.2	31.2	31.2	31.8	31.8	xx	33.3	33.2	33.2	34.2	34.2	34.2	33.1
H	28.3	31.2	31.2	31.2	31.8	31.8	33.3	33.3	33.2	33.2	34.2	34.2	34.2	33.1
I	27.5	30.2	xx	31.5	31.5	31.5	31.8	31.8	33.7	33.7	33.7	xx	33.5	32.4
J	27.5	30.2	31.5	31.5	xx	31.5	31.8	31.8	33.7	xx	33.7	33.7	33.5	32.4
K	27.5	28.3	31.5	31.5	31.5	31.5	31.1	31.1	33.7	33.7	33.7	33.7	31.8	32.4
L	26.0	28.3	xx	31.5	31.5	xx	31.1	31.1	xx	33.7	33.7	xx	31.8	30.0
M	26.0	38.3	28.3	28.3	30.0	30.0	31.1	31.1	31.7	31.7	31.8	31.8	31.8	30.0
N	26.0	26.0	26.0	27.2	27.2	27.2	27.9	27.9	28.6	28.6	28.6	30.0	30.0	30.0

Figure 4: Pin by pin fuel rod burn up distribution of the assembly C15

	1	2	3	4	5	6	7	8	9	10	11	12	13	14
A	28.2	27.8	27.5	27.3	27.1	27.0	26.9	25.4	25.3	25.0	25.0	24.0	23.2	22.3
B	29.6	29.5	29.7	29.1	28.9	29.2	28.7	27.1	27.4	26.8	26.3	26.0	24.8	23.6
C	31.0	31.4	xx	31.3	31.1	xx	30.7	29.0	xx	28.8	28.3	xx	26.5	24.8
D	32.1	32.2	32.8	32.5	32.8	32.5	31.5	29.6	30.3	30.2	29.3	28.7	27.2	25.8
E	33.2	33.4	34.0	34.2	xx	33.4	32.4	30.1	30.9	xx	30.7	29.7	28.1	26.7
F	34.3	34.9	xx	35.0	34.5	34.0	34.0	30.9	30.9	31.3	31.2	xx	29.2	27.4
G	35.1	35.2	35.7	34.9	34.4	34.9	xx	31.8	31.0	30.9	30.9	30.7	29.3	27.9
H	36.2	36.3	36.8	35.9	35.2	34.9	35.0	34.4	33.8	33.6	33.5	33.3	31.7	30.3
I	37.0	37.7	xx	37.8	37.0	35.8	34.9	34.7	34.8	35.2	35.1	xx	32.8	30.9
J	37.7	38.0	38.7	38.8	xx	37.4	35.9	35.5	36.3	xx	36.0	34.8	32.9	31.4
K	38.5	38.7	39.4	39.0	39.2	38.6	37.2	36.8	37.6	37.3	36.2	35.4	33.6	32.1
L	39.2	39.9	xx	39.8	39.5	xx	38.6	38.2	xx	37.7	37.0	xx	34.8	32.9
M	39.7	39.8	40.2	39.4	39.1	39.3	38.4	38.2	38.5	37.5	36.9	36.6	35.0	33.6
N	40.3	40.0	39.7	39.4	39.1	38.8	38.5	38.6	38.3	37.8	37.2	36.5	35.5	34.6

Figure 5: Pin by pin fuel rod burn up distribution of the assembly G23

	1	2	3	4	5	6	7	8	9	10	11	12	13	14
A	35.7	35.7	35.8	35.8	35.9	36.0	35.9	35.8	35.8	35.9	36.0	36.3	36.6	37.1
B	36.0	36.4	37.1	36.7	36.7	37.3	36.8	36.6	37.2	36.8	36.9	37.6	37.3	37.4
C	36.3	37.3	xx	37.9	38.0	xx	37.9	37.7	xx	38.1	38.2	xx	38.3	37.7
D	36.5	37.0	38.1	38.1	38.7	38.6	37.5	37.4	38.4	38.7	38.3	38.6	38.0	37.9
E	36.6	37.2	38.3	38.8	xx	38.3	37.3	37.0	38.1	xx	39.0	38.8	38.1	38.0
F	36.7	37.7	xx	38.6	38.3	37.9	38.0	37.2	37.2	38.1	38.8	xx	38.7	38.1
G	36.6	37.1	38.0	37.5	37.2	37.9	xx	37.6	36.6	36.9	37.7	38.6	38.1	38.0
H	36.5	37.0	37.9	37.4	37.0	37.1	37.6	36.8	36.5	36.8	37.6	38.5	38.0	37.9
I	36.5	37.6	xx	38.4	38.0	37.1	36.6	36.4	36.9	38.0	38.7	xx	38.5	37.9
J	36.4	37.0	38.1	38.5	xx	37.9	36.8	36.7	37.8	xx	38.8	38.7	38.0	37.8
K	36.3	36.9	37.9	37.9	38.5	38.3	37.3	37.2	38.3	38.6	38.2	38.5	37.9	37.7
L	36.3	37.3	xx	37.9	38.0	xx	37.8	37.7	xx	38.1	38.2	xx	38.9	37.7
M	36.1	36.5	37.2	36.8	36.9	37.4	36.9	36.8	37.4	36.9	37.1	37.8	37.4	37.5
N	36.0	36.0	36.2	36.2	36.2	36.3	36.3	36.2	36.2	36.3	36.4	36.7	36.9	37.4

Figure 6: Pin by pin fuel rod burn up distribution of the assembly J14

DATA ACQUISITION

Neutron measurement experiments were conducted using a miniature neutron detector which was placed into a thin stainless steel tube. The fission chamber was commercially available from Centronic and it had a diameter of 6.3 mm. This tube was inserted, in turn, into each of the guide tubes for neutron measurements, generating 16 pulse height spectra for each assembly. The measurement data were obtained in a pulse height spectrum format with 1024 channels. All measurements were obtained at 150 cm below from the top of the fuel assembly with the measurement time of 100 seconds. In addition, a total of 11 spectra were obtained at multiple depths at the guide tube position L-12 of the assembly J14 to measure neutron and gamma radiation levels. The measurements were taken with MMCA (Mini Multi-Channel Analyzer), the standard IAEA MCA, and WinSPEC, one of the standard pieces of software at the Department of Safeguards at IAEA. The main advantage of using this hardware and software is that there would be no training required for IAEA inspectors as the electronics and the software are already being widely used at IAEA.

RESULTS AND DISCUSSION

To obtain neutron counts, a threshold was applied to all measured spectra at channel 200 which was high enough to ensure that no gamma pile up effect was influencing the neutron counts. The axial neutron and gamma profiles taken from the fuel assembly J14 at the position L12 are shown in Figure 7. As the measurement position moves deeper, the neutron as well as gamma radiation level increases. The reduction of the neutron level at 150 cm is due to the presence of the grid near this depth.

Table 2 shows both experimental neutron data and MCNP simulated data which are normalized to the maximum value of the each assembly, as well as the raw data for measurements. Figures 8-10 show the comparison between the experimental data and simulated data for all three assemblies. For the most part the MCNP and experimental data were within 0.05 of each other with a small number agreeing within 0.1. Overall, it is concluded that the MCNP simulated data agreed extremely well with the measured data, thus providing good validation of the simulation methodology.

Note on the plot and error bars: The statistical uncertainty at the 1- σ level for the ratio is between 1 and 2 percent for the MCNP simulation. All measurement errors are less than 5%. For the sake of clarity, the statistical uncertainties and the measurement errors are not shown in these subsequent plots. Figure 8 is shown with error bars for an example.

On the safeguards verification note, an inspector can easily conclude that the PWR spent fuel assembly C15 is disturbed without even having the detailed knowledge of the C15 assembly as the measured neutron signature severely deviated from the expected neutron signature (base signature in green color) which is cyclic and symmetric. The inspector can also suspect that the spent fuel rods in the 4th quadrant are quite different from the rest of the fuel rods arrangement as there were increases in the neutron flux in the 4th quadrant. Note that the amount of diversion in this case was 12% whereas the current IAEA criterion for partial defect testing is 50%. For verification of G23, the neutron profile also deviated from the neutron base profile and it lacked the smooth symmetric pattern, an indication of disruption of the fuel integrity. For J14, the deviation of the neutron is only slight for the data point E5, but it kept the smooth repetitive symmetric pattern in essence.

On an interesting note, close observation of Figure 10 discloses that the only difference between the measured plot and simulated plot is in the location of the highest peak. Investigation revealed that the facility staff erroneously reported the missing pin location at E11 rather than its true location at D5. As the MCNP simulation was performed with the data provided by the facility, the location of the peak obtained by measurements did not match the simulation profile. Although this small error was relatively

less important in terms of material accounting, this finding demonstrates the effectiveness of the methodology, and the instrument, when available, could be potentially a very powerful tool for IAEA inspectors for verification of a spent fuel assembly to the partial defect level. Note that the neutron measurement was sensitive enough to identify the scenario of the single pin missing, at least in this case, whereas the existing tool cannot even tell if 50% of the spent fuel is missing or replaced with dummy fuel pins.

A MCNP case was run on the J14 with the corrected information that the missing location was at D5. The neutron profile obtained with this new MCNP matched very well with the measured neutron profile as shown in Figure 11.

Table 2: Neutron measurement and MCNP simulated data for the assembly C-15, G23 and J14. The experimental data were obtained with the measurement time of 100 seconds. Relative values are individual signals normalized to the maximum signal

Detector Position	Neutron Measurement: C15		Simulation Data	Neutron Measurement: G23		Simulation Data	Neutron Measurement: J14		Simulation Data
	Raw 100 s	Rel. Value	Rel. Value	Raw 100 s	Rel. Value	Rel. Value	Raw 100 s	Rel. Value	Rel. Value
J5	555	0.38	0.41	1097	0.89	0.84	1343	0.85	0.87
I3	554	0.38	0.38	1184	0.96	0.89	1304	0.83	0.81
L3	401	0.27	0.32	1170	0.94	1.00	1084	0.69	0.71
L6	553	0.38	0.39	1030	0.83	0.77	1291	0.82	0.81
J10	606	0.41	0.43	1239	1.00	0.97	1410	0.90	0.87
L9	562	0.38	0.39	1010	0.82	0.81	1299	0.83	0.81
L12	470	0.32	0.34	866	0.70	0.63	1108	0.71	0.71
I12	626	0.43	0.40	912	0.74	0.68	1271	0.81	0.82
E5	674	0.46	0.42	994	0.80	0.69	1571	1.00	0.88
C6	617	0.42	0.42	892	0.72	0.66	1387	0.88	0.81
C3	553	0.38	0.38	700	0.56	0.53	1165	0.74	0.71
F3	592	0.40	0.39	1009	0.81	0.81	1330	0.85	0.82
E10	1462	1.00	1.00	870	0.70	0.65	1436	0.91	1.00
F12	1193	0.82	0.75	794	0.64	0.57	1305	0.83	0.88
C12	1339	0.92	0.90	755	0.61	0.53	1122	0.71	0.73
C9	866	0.59	0.58	951	0.77	0.76	1285	0.82	0.82

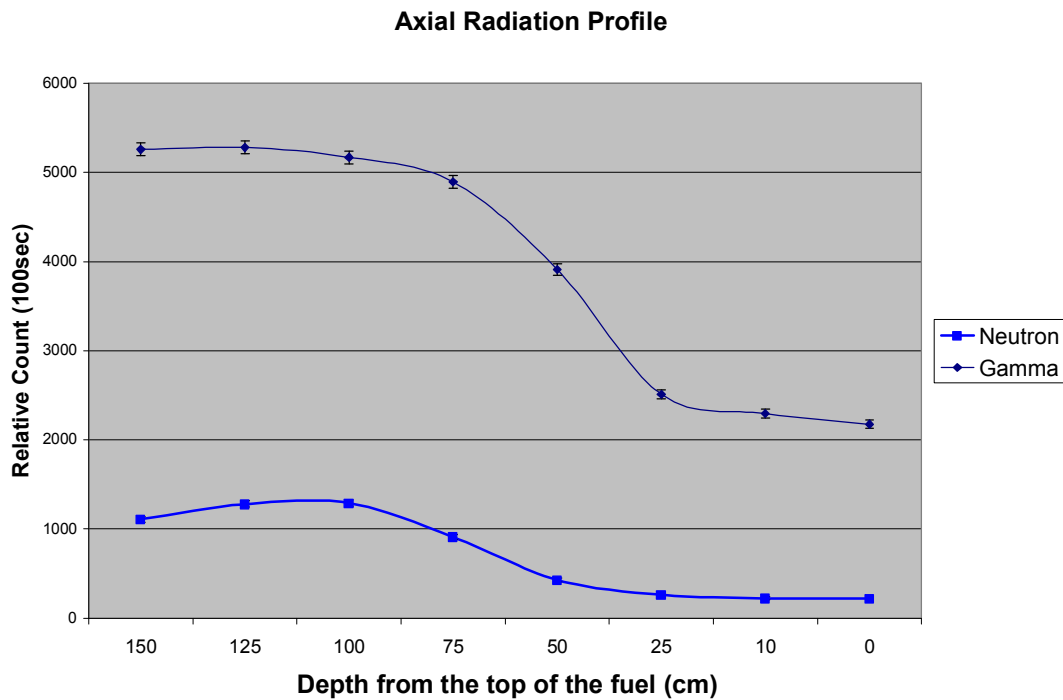


Figure 7: Axial neutron profile of the spent fuel assembly J14 at the position L12.

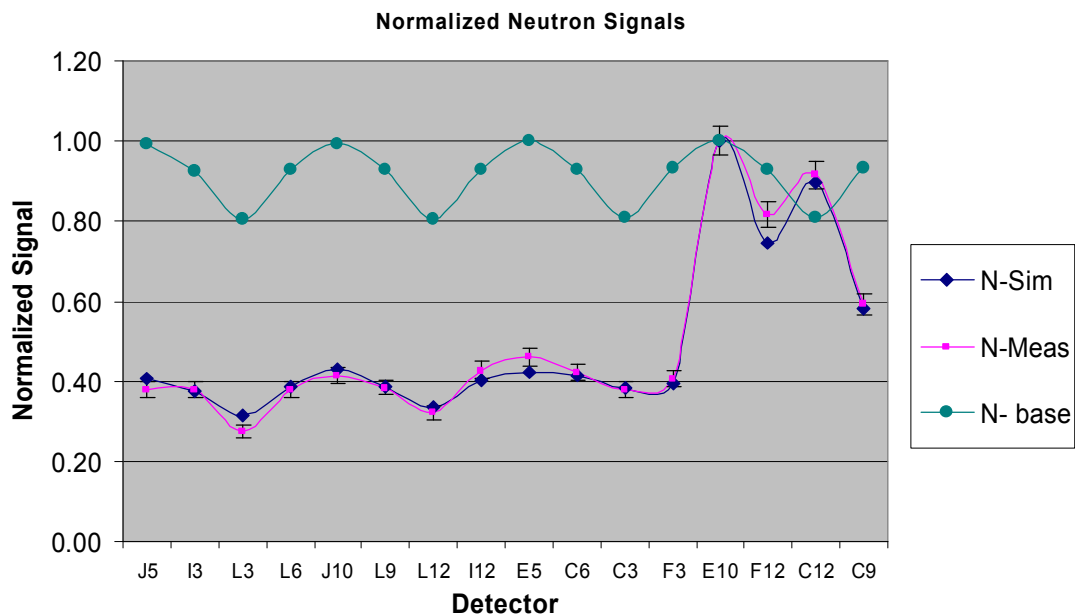


Figure 8: Comparison of the experimental neutron data to the MCNP simulated data for the assembly C15. The N-base profile shows the case where there was no diversion. The measured signature shows the deviation from the N-base profile leading to conclusion that the assembly C15 was tampered from the original status.

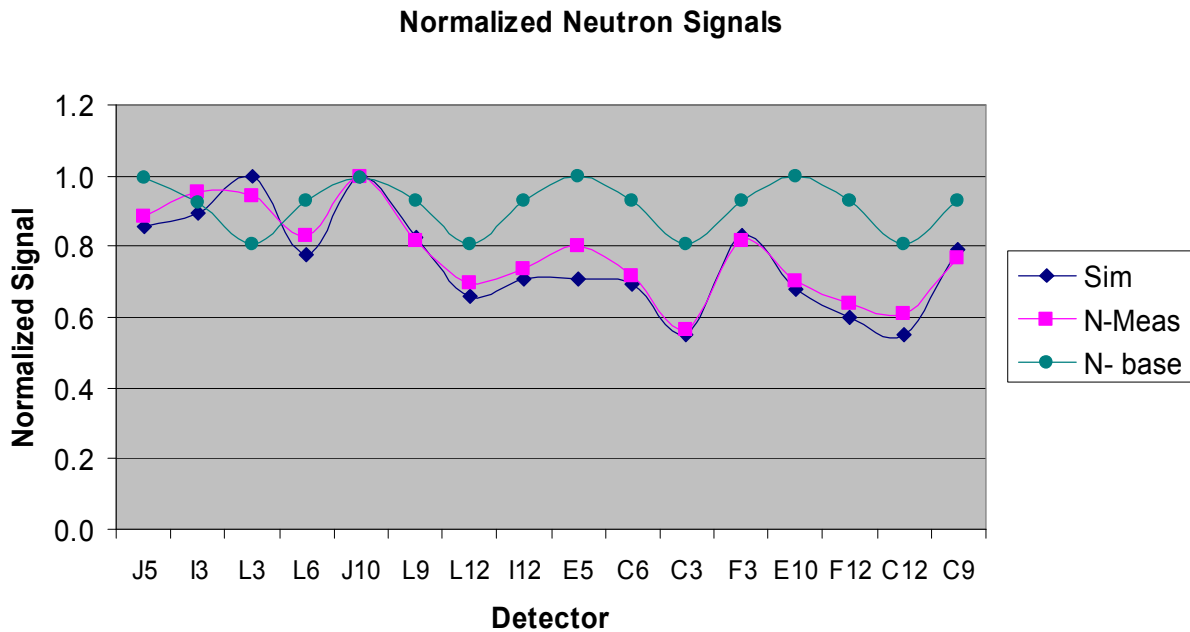


Figure 9: Comparison of the experimental neutron data to the MCNP simulated data for the assembly G23

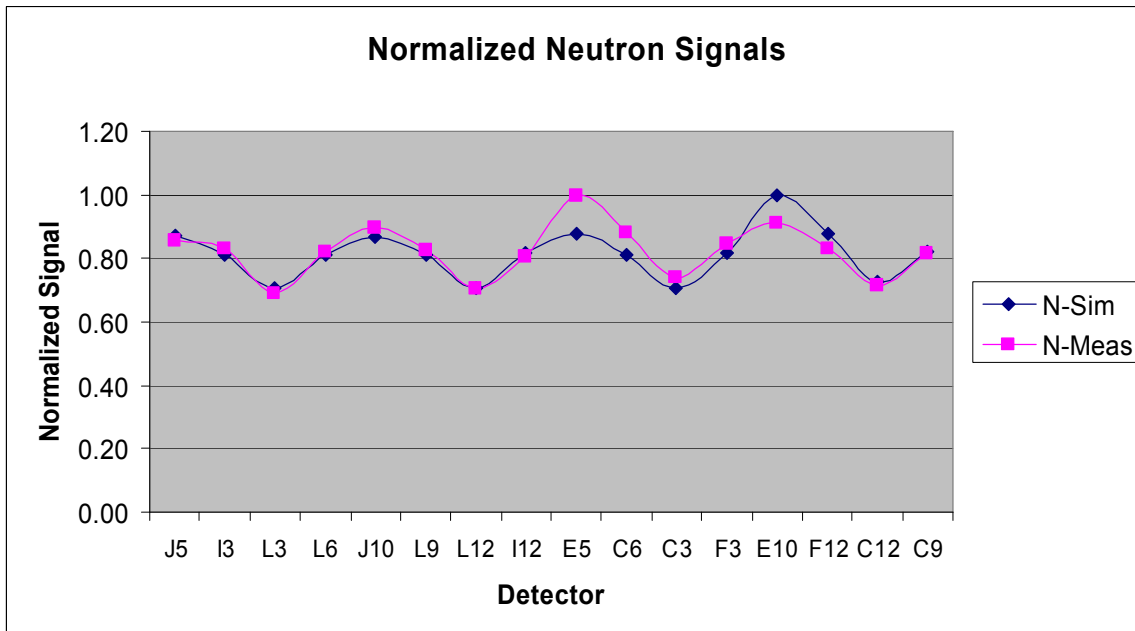


Figure 10: Comparison of the experimental neutron data to the MCNP simulated data for the assembly J14. The discrepancy between the MCNP simulated data and measurement data were caused by the misreport of the removed fuel pin location by the facility operator. The actual position of the removed pin was right next to E5 rather than the position next to E10.

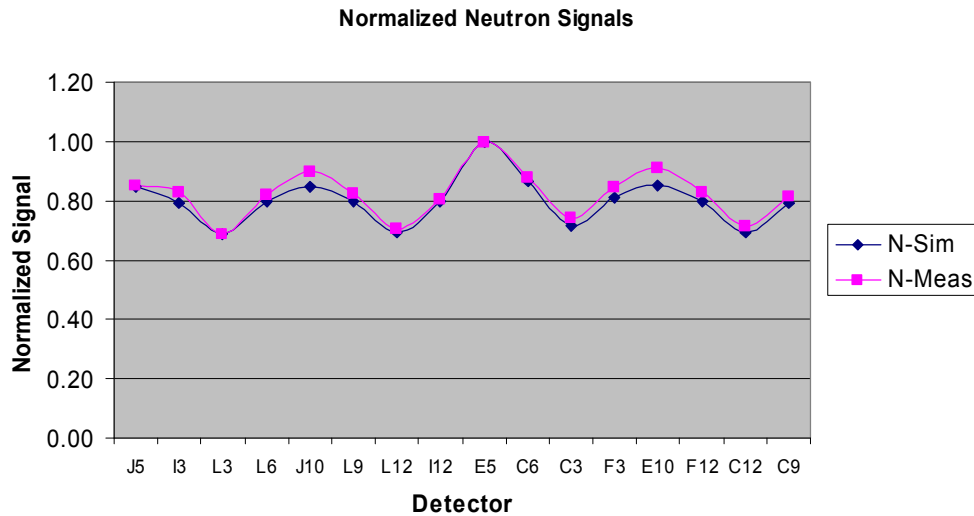


Figure 11: Comparison of the experimental neutron data to the MCNP simulated data for the assembly J14. The new MCNP result was obtained with the corrected mission rod location. They matched fairly well.

CONCLUSION

Benchmarking experiments have been performed to demonstrate that the pin diversion detection methodology can be used for partial defect verification of the PWR spent fuel assemblies without operator declared data. The results from the experiments were compared with the simulations and the agreement between the two was well within ten percent. Thus, based on the simulation studies and benchmarking measurements, the methodology developed promises to be a powerful and practical way to detect partial defects that constitute 10% or more of the total active fuel pins. This far exceeds the detection threshold of 50% missing pins from a spent fuel assembly, a threshold defined by the IAEA Safeguards Criteria.

REFERENCES

- [1] Y. Ham, G. I. Maldonado, C. Yin, J. Burdo, "Monte Carlo Characterization of Pressurized Water Reactor Spent Fuel Assembly for Development of a New Instrument for Pin Diversion Detection," Institute of Nuclear Materials Management 47th Annual Meeting, Nashville, TN, July 2006.
- [2] Y. Ham, G. I. Maldonado, J. Burdo, T. He "Development of a Safeguards Verification Method and Instrument to Detect Pin Diversion from PWR Spent Fuel Assemblies," Symposium on International Safeguards, Vienna, Austria, 16-20 October, 2006
- [3] Sitaraman, S. and Ham, Y., "Characterization of a Safeguards Verification Methodology to Detect Pin Diversion from Pressurized Water Reactor (PWR) Spent Fuel Assemblies using Monte Carlo Techniques," Proceedings of the INMM 48th Annual Meeting, Tucson, AZ, July 2007.
- [4] S. Sitaraman and Y.S. Ham, "Sensitivity Studies for an In-Situ Partial Defect Detector (PDET) in Spent Fuel using Monte Carlo Techniques", 49th Annual Meeting of the Institute of Nuclear Materials Management, Nashville, TN, July 2008.
- [5] S. Sitaraman and Y.S. Ham, "Symmetric Pin Diversion Detection using a Partial Defect Detector (PDET)," 50th Annual Meeting of the Institute of Nuclear Materials Management, Tucson, Arizona, July 2009.